Three-dimensional passive acoustic tracking of sperm whales (Physeter macrocephalus) in ray-refracting environments

Aaron Thode and WWA

Citation: The Journal of the Acoustical Society of America **118**, 3575 (2005); doi: 10.1121/1.2049068
View online: http://dx.doi.org/10.1121/1.2049068
View Table of Contents: http://asa.scitation.org/toc/jas/118/6
Published by the Acoustical Society of America

Three-dimensional passive acoustic tracking of sperm whales (*Physeter macrocephalus*) in ray-refracting environments

Aaron Thode[a)]
Marine Physical Laboratory, Scripps Institution of Oceanography, San Diego, California 92093-0205

(Received 8 April 2005; revised 3 August 2005; accepted 11 August 2005)

A wide-aperture towed passive acoustic array is used to obtain ranges and depths of acoustically active sperm whales in the Gulf of Mexico in June 2004, by extending a technique previously reported [Thode, J. Acoust. Soc. Am. **116**, 245–253 (2004)] to explicitly account for ray-refraction effects arising from a depth-dependent sound speed profile. Under this expanded approach, three quantities are measured from an impulsive sound: the time difference between direct-path arrivals on a forward and rear subarray, the time difference between the direct and surface-reflected paths on the rear subarray, and the acoustic bearing measured on the rear subarray. These quantities, combined with independent measurements of hydrophone depths and cable inclination, are converted into range-depth position fixes by implementing an efficient numerical procedure that uses a ray-tracing code to account for ray-refraction effects caused by depth-dependent sound speed profiles. Analytic expressions that assume a constant waterborne sound speed are also derived. Foraging depths of various sperm whales over 10 days in June, 2004 are estimated using the numerical technique. © *2005 Acoustical Society of America.*
[DOI: 10.1121/1.2049068]

PACS number(s): 43.30.Sf, 43.80.Ka [WWA] Pages: 3575–3584

I. INTRODUCTION

Sperm whales are a vocally active species, and detecting their signals, or "clicks," using towed passive acoustic arrays has become a standard procedure for detecting, locating, and monitoring these animals.[1,2] The seismic exploration industry is considering implementing passive acoustic monitoring systems as part of standard mitigation procedures during deep-water seismic exploration, due to concerns about the potential effects of deep-water airgun activity on deep-diving marine mammals such as the sperm whale.[3]

Most passive array systems have the ability to estimate a sound's bearing relative to the tow cable axis. They achieve this by measuring the signal's arrival time difference between two hydrophones spaced a few meters apart, and then assuming a planar wave front, yielding a monotonic relationship between arrival time difference and arrival angle. Using a single short-aperture array, the range to an animal can then be estimated by measuring how the measured bearings from a particular animal shift over time while the observation platform is moving.[1,2,4] If the velocity of the platform is much greater than that of the animal, then a time-motion analysis will yield a set of bearings that intersect at an animal's range over a 3–10 minute interval.

Unfortunately, typical seismic vessels operational speeds of 1–2 m/s are not much greater than estimated sperm whale swimming speeds,[5,6] invalidating the assumptions of time-motion analysis. Furthermore, obtaining a range estimate via this approach usually requires several minutes of continuous vocalizing, and assumes that individuals vocalizing simultaneously can clearly be distinguished, conditions which are not always met. Other algorithms assume that measuring the received level of a signal, and comparing this level to a reference database of typical source levels, can provide a range estimate. However, data on source levels are scarce, individuals can create sounds with varying source levels, and several marine mammal sounds, including sperm whale sounds, are now understood to be highly directional.[7–9] Thus at present there is no reliable way to range sperm whales, or any broadband biological underwater sound, using standard acoustic monitoring and mitigation equipment.

The situation is even more difficult for certain species of deep-diving mammals, including sperm and beaked whales, as a deep animal's depth must be determined in order to distinguish the "slant range," or the distance between the array and the animal, from the "horizontal range," or horizontal separation between the array and the animal. For directional sources like seismic airgun arrays this distinction may be important—the received sound level obtained by an animal 1 km directly below a towed airgun array is predicted to be 20 dB rms greater from that received by an animal at 1 km horizontal range,[10,11] even though the slant ranges for both animals would be the same.

In 2003 the US Minerals Management Service (MMS) and the Industry Research Funders Coalition supported efforts to develop a three-dimensional (3D) passive acoustic tracking method for sperm whales, by exploiting surface-reflected acoustic arrivals to create a virtual planar array out of a large-aperture towed array. During 2003 the Sperm Whale Seismic Study (SWSS) conducted a research cruise in the Gulf of Mexico, and the tracking concept was demonstrated using data collected from an autonomous recorder attached to the end of a short-aperture towed array. The analysis of this data has been previously reported.[12] If the

a)Electronic mail: thode@mpl.ucsd.edu

horizontal separation between two widely spaced hydrophones was at least 200 m, range/depth estimates could be obtained from sperm whale clicks out to 1 km horizontal range. Bottom-reflected acoustic multipath were not required for tracking, but when bottom returns were detected they provided an independent confirmation of the tracking procedure.[8]

The two-hydrophone analytic method presented in Ref. 12, however, suffers from two weaknesses. The first is that a surface-reflected path must be recorded on both hydrophones. Whenever this situation occurs, it permits a simple and straightforward analytical solution, but under many practical circumstances noise from the towing vessel may degrade or eliminate the ability to detect surface reflections on the hydrophones closest to the ship. A more serious limitation is that the assumption of a uniform spatially independent waterborne sound speed limits the accuracy of the method to ranges of 1 km or less in regions like the Gulf of Mexico, where stratified conditions produce strongly depth-dependent sound speed profiles. These profiles can cause substantial ray refraction of both direct and surface-reflected paths when the initial propagation angle of the departing acoustic energy lies close to the horizontal, and thus the rectilinear approximations behind the analytical formulas are violated.

Both problems were encountered during the 2004 SWSS field season, when data were collected from a tandem towed-array system constructed specifically for passive acoustic range-depth tracking. The surface-reflected paths were difficult to detect on the hydrophones closest to the ship, due to self-noise from the ship's propeller. Thus Sec. II presents a new analytic solution that only requires surface-reflected paths to be detected on one hydrophone, but requires an estimate of the acoustic bearing of a signal at the same hydrophone. The new tracking solution also has the advantage of being more robust to uncertainties in hydrophone depth. However, the new formulas in Sec. II still neglect the potential effects of ray refraction due to a depth-dependent sound speed profile, so in Sec. III numerical procedures for incorporating refraction effects are presented. Section IV presents details of the experimental deployment and automated data analyses, discusses how the tracking hardware and procedures were tested using data from June 16, 2004, and concludes with estimates of foraging depths of several animals over several days in the Gulf of Mexico.

II. ANALYTICAL TRACKING SOLUTION

An analytical solution for a 3D whale position can be obtained if a constant underwater sound speed is assumed, and thus ray paths are rectilinear. In Sec. III this assumption is dropped and the effects of a depth-dependent sound speed profile are incorporated into a numerical tracking procedure.

The geometry and parameters of the required array system are illustrated and defined in Fig. 1, and an example of a realistic tow configuration is shown in Fig. 2. Along a single towed array cable four array elements are arranged as two short-aperture subarrays separated by a cable distance L, with the forward subarray at a depth $z_{a,f}$ and the rear subarray at a depth $z_{a,r}$. In all future expressions, "f" or "r" subscripts designate measurements at the forward or rear subarray, respectively, and i designates a dummy variable that can represent either location. It is assumed that the cable lies in a two-dimensional plane perpendicular to the ocean surface, e.g., the ship is not turning and current velocity is depth independent. The separation between the two elements in each subarray is small enough that any signal wave front moving across the array aperture can be modeled as a plane wave (i.e., a Fraunhoffer approximation). Thus the bearing of a direct-path signal relative to the array cable, $\eta_{d,I}$, can be defined and estimated at both subarrays using standard cross-

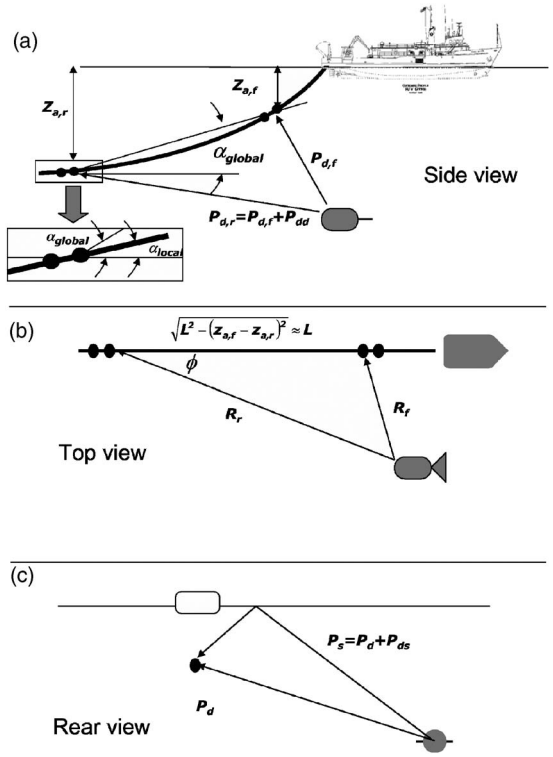

FIG. 1. Schematic of tandem array deployment geometry, defining symbols used in Sec. II, (a) side view of system; inset, expanded view of rear subarray illustrating the difference between the local tilt α_{local} and global cable inclination α_{global}. (b) Top view of system illustrating horizontal ranges; (c) rear view looking forward, illustrating notation for direct and surface-reflected paths.

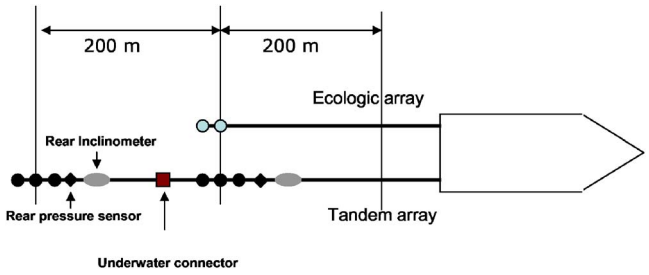

FIG. 2. Illustration of 3D deployment off R/V Gyre in 2004, viewed from above. The tandem array deployed off the starboard stern was specifically built for the project, and consisted of two subarrays separated by 200 m, each subarray consisting of three hydrophones and a pressure transducer. The tandem array and a second (Ecologic) array were deployed in parallel, permitting bearings of sounds to be determined without a port/starboard ambiguity. Round circle, calibrated hydrophone; diamonds, pressure (depth) sensors; oval, autonomous inclinometer package; square, underwater connector.

correlation methods. The formulas presented here use only $\eta_{d,r}$, or the bearing measured from the rear subarray, to minimize potential signal masking from ship noise interference.

A whale position is specified by the coordinates (R_i, z_w, ϕ_i) for the whale's horizontal range, depth, and azimuth from subarray i, respectively, where $\phi=0$ represents a position directly ahead of the ship. The "slant range" traveled by a sound along the direct propagation path to a given subarray i is $P_{d,i}=\sqrt{R_i^2+(z_w-z_{a,i})^2}$, and the distance traveled along the surface-reflected path to the same subarray is $P_{s,i}=\sqrt{R_i^2+(z_w+z_{a,i})^2}$. From these two expressions one obtains the useful formula

$$z_w = \frac{P_{ds,r}(2P_{d,f}+2P_{dd}+P_{ds,r})}{4z_{a,r}}, \tag{1}$$

where $P_{ds,r}=P_{s,r}-P_{d,r}$ is the difference between the direct and surface-reflected paths on the rear subarray, and the difference between the direct path slant ranges at the forward and rear locations is defined by $P_{dd}=P_{d,r}-P_{d,f}$. From estimates of $P_{ds,r}$, P_{dd}, and $\eta_{d,r}$ it should be possible to derive the whale's spatial coordinates. The first two estimates can be derived by measuring the relative arrival times $t_{ds,r}$ and t_{dd} and converting them to path length differences using an effective medium sound speed c. Estimates of $P_{ds,f}$ and $\eta_{d,f}$ will not be required in the derivation, anticipating the realities of noise contamination on the forward subarray. However, whenever these quantities are measurable, they can be used to verify the position fix.

Besides knowledge of both subarray tow depths, some additional ancillary measurements of the towed array cable are needed. In particular, information about the cable vertical inclination and curvature, or "sag," must be incorporated, in the form of a "local" tilt and "global" tilt. The rear subarray local tilt α_{local} is the angle between a horizontal line and a line connecting the two rear subarray elements [Fig. 1(a)]. The global tilt α_{global} is the angle between the horizontal line and a line connecting the front elements of the front and rear subarrays, or $\alpha_{\text{global}}=\sin^{-1}[(z_{a,r}-z_{a,f})/L]$. If the array cable has no sag, then the local and global tilt angles will be equal.

The relationship between an animal's azimuth, local tilt, and direct-path bearing $\eta_{d,r}$ is governed by

$$\cos\,\eta_{d,r} = \cos\,\phi\,\cos\,\alpha_{\text{local},r}\,\sin\,\theta_{d,r} + \sin\,\alpha_{\text{local},r}\,\cos\,\theta_{d,r}, \tag{2}$$

where $\theta_{d,r}$ is the elevation angle of the direct-path arrival on the rear subarray, defined relative to the upward z axis such that $\cos\,\theta_{d,r}=(z_{a,r}-z_w)/P_{d,r}$ and $\sin\,\theta_{d,r}=R_r/P_{d,r}$.

From the law of cosines a relationship between the forward and rear slant ranges can be obtained

$$P_{d,f}^2 = L^2 + P_{d,r}^2 - 2LP_{d,r}\cos\,\eta_{\text{global}} \tag{3}$$

with

$$\cos\,\eta_{\text{global}} = \cos\,\phi\,\cos\,\alpha_{\text{global}}\,\sin\,\theta_{d,r} + \sin\,\alpha_{\text{global}}\,\cos\,\theta_{d,r}. \tag{4}$$

Substituting Eqs. (2)–(4) into Eq. (1) one obtains an expression for the rear slant range,

$$P_{d,r} = P_{dd} + \frac{LP_{dd}\cos\,\alpha_{\text{global}}\cos\,\eta_{d,r} - \cos\,\alpha_{\text{local},r}(L^2+P_{dd}^2)/2 - L\,\sin(\alpha_{\text{local},r}-\alpha_{\text{global}})[z_{a,r}-P_{ds,r}(2P_{dd}+P_{ds,r})/4z_{a,r}]}{\cos\,\alpha_{\text{local},r}P_{dd} - L\cos\,\eta_{d,r}\cos\,\alpha_{\text{global}} - LP_{ds,r}\sin(\alpha_{\text{local},r}-\alpha_{\text{global}})/z_{a,r}}. \tag{5}$$

For the special case where the array cable is straight, or $\alpha_{\text{global}}=\alpha_{\text{local}}$, one finds

$$P_{d,r} = P_{dd} + \frac{LP_{dd}\cos\,\eta_{d,r} - (L^2+P_{dd}^2)/2}{P_{dd} - L\cos\,\eta_{d,r}}. \tag{6}$$

Substituting $P_{d,r}$ into Eq. (1) yields the whale depth, from which the range R_r and azimuth ϕ_r can be derived. Thus if independent estimates of $z_{a,f}, z_{a,r}$ and the local array tilt α_{local} are available, the whale position may be obtained by measuring the relative arrival times of a direct-path arrival between subarrays, and relative arrival times between the direct- and surface-reflected-path arrivals on the rear subarray alone.

The denominator of Eq. (6) indicates that in order for the slant range to be finite the signal wave front across aperture L must have significant curvature (i.e., be in the Fresnel zone). Alternatively stated, the bearings of the signal measured between the forward and rear subarrays must be sufficiently different to allow the animal's slant range to be calculated, even though the procedure here does not explicitly incorporate the forward subarray bearing. A general rule of thumb is that if the hydrophone elements are separated by a distance L then a broadside slant range of $5-10L$ should be resolvable.[13]

To estimate the inverted location uncertainties, a sensitivity analysis for the technique was conducted for a whale located at 1 km range and 400 m depth, using representative subarray depths and $L=200$ m (Table I). The 1 km range corresponds to the expected outer limit of the tracking algorithm for this subarray separation. Each of the input parameters was varied by an amount representative of the typical uncertainty of that measurement, 1 ms for relative time-of-arrival measurements, 1 m for subarray depth measurements, and up to 1 degree for the local tilt measurements. The spread in output values indicates that a whale depth can be estimated to within ±50 m, with most of the uncertainty dominated by imprecise estimates of t_{dd} and α_{local}. The impact of the local tilt is particularly felt whenever the whale's azimuth moves toward 0° or 180°. If $L=500$ m these depth uncertainties drop to ±20 m.

TABLE I. Sensitivity of analytic tracking algorithm to input uncertainties. Forward and rear subarray depths are 30 m and 50 m, respectively, with local tilt of 3 degrees on rear subarray.

Perturbation	Horizontal range (R_r) in m	Whale depth (z_w) in m
Baseline (L=200 m, ϕ_R=90°)	1000	400
Increase $t_{ds,r}$ by 1 ms	1002	420
Increase t_{dd} by 1 ms	1090	436
Increase $z_{a,R}$ by 1 m	1016	397
Increase α_{local} 1 degree	940	376
Baseline (L=200 m, ϕ_R=25°)	1000	400
Increase $t_{ds,r}$ by 1 ms	1016	425
Increase t_{dd} by 1 ms	1231	492
Increase $z_{a,R}$ by 1 m	1052	411
Increase α_{local} 1 degree	845	338

III. NUMERICAL TRACKING PROCEDURE

The localization formulas in Eqs. (1), (5), and (6) neglect potential ray refraction effects caused by depth-dependent sound speed profiles in the Gulf of Mexico. To explicitly account for these effects, a numerical procedure was created that implements a standard ray-tracing propagation code to compute the travel times, elevation angles, and t_{ds} values produced by a set of impulsive sources placed along a grid of horizontal ranges and depths. The most straightforward approach to implementing the algorithm would be to compute and store the ray paths and travel times of sources arranged along a three-dimensional grid surrounding the tandem towed array system, and then to construct an error function that indicates the mismatch between the measured relative arrival times and arrival angles with the modeled arrival times and angles. The 3D location that generates the error minimum would be chosen as the true location. This "matched-field" processing approach has been successfully demonstrated on large-aperture distributed array systems, where the sensors are permanently mounted on the ocean floor.[14,15] The problem with this approach when applied to the current situation is the dynamic nature of the array geometry. The towed array depths are constantly changing with time, and thus ray computations of all possible combinations of the 3D source locations and receiver depths becomes daunting.

Fortunately the problem can be reduced to a two-dimensional grid search over range and depth by using the ray-tracing code to precompute three L by M by N matrices, which represent a grid of L depths, M ranges, and N receiver depths. Thus the modeled values at the l,m,n coordinate represent an impulsive source at depth z_l and range R_m propagating to a receiver at depth z_n. The first matrix contains the computed travel distance $\mathbf{P_d}$ between the source and receiver combinations, the second matrix contains the elevation angle $\boldsymbol{\theta}_\mathbf{d}$ measured at the receiver, with the elevation angle defined as in Eq. (2), and the third matrix contains $\mathbf{t_{ds}}$, the modeled arrival-time difference between the direct and surface-reflected ray paths, t_{ds}.

For each measurement of t_{dd}, $t_{ds,r}$, and η_d, the following steps are taken:

(1) The receiver depth z_n that best matches the measured depth of the rear subarray, $z_{a,r}$, is used to extract the appropriate L by M matrices $\mathbf{P_d}(z_{a,r})$, $\boldsymbol{\theta}_\mathbf{d}(z_{a,r})$, and $\mathbf{t_{ds}}(z_{a,r})$. The matrix $\mathbf{P_d}(z_{a,f})$ that corresponds with the forward subarray depth $z_{a,f}$ is also extracted.
(2) A grid search along source depth z_l is conducted. For each value of z_l, the following steps are performed.
  (a) Interpolate along R_m to find a modeled value of $t_{ds,lm}=\mathbf{t_{ds}}(z_l,R_m,z_{a,r})$ that best matches the measured $t_{ds,r}$. Determine the corresponding interpolated values of $\theta_{d,lm}=\boldsymbol{\theta}_\mathbf{d}(z_l,R_m,z_{a,r})$, and $P_{d,lm}=\mathbf{P_d}(z_l,R_m,z_{a,r})$ for this interpolated range $R_{m,r}$.
  (b) Estimate the source azimuth relative to the rear subarray by rearranging Eq. (2),

$$\cos\phi^{(1)}=\frac{\cos\eta_{d,r}-\sin\alpha_{\text{local},r}\cos\theta_{d,lm}}{\cos\alpha_{\text{local},r}\sin\theta_{d,lm}}. \tag{7a}$$

  (c) Interpolate along R_m to find a modeled value of $\mathbf{P_d}(z_l,R_m,z_{a,f})$ that best matches $P_{d,lm}-P_{dd}$, and assign a value of $R_{m,f}$ to this range.
  (d) Make a second estimate of source azimuth using the law of cosines relationship

$$\cos\phi^{(2)}=\frac{R_{m,f}^2-L^2-R_{m,r}^2}{2LR_{m,r}}. \tag{7b}$$

  (e) Define an error function $E(z_l)=\cos\phi^{(2)}-\cos\phi^{(1)}$.
(3) Interpolate along $E(z_l)$ to find the modeled source depth z_l^* such that $E(z_l^*)=0$.
(4) Repeat steps (2a) and (2b) to obtain the best-fit source range and azimuth.

The top subplot of Fig. 3 shows a typical sound speed profile in the Gulf of Mexico (GOM) acquired from CTD casts during June, 2004. Generally, the sound speed profile was very stable with only slight changes over a 3 week period. The downward-refracting tendency of this environment is clearly indicated by the monotonic decrease of the water sound speed from over 1540 m/s at the surface to 1490 m/s at the bottom. The next three subplots show contour plots of ray path length P_d, arrival time differences between the direct and surface-reflected path t_{ds}, and elevation angle for a

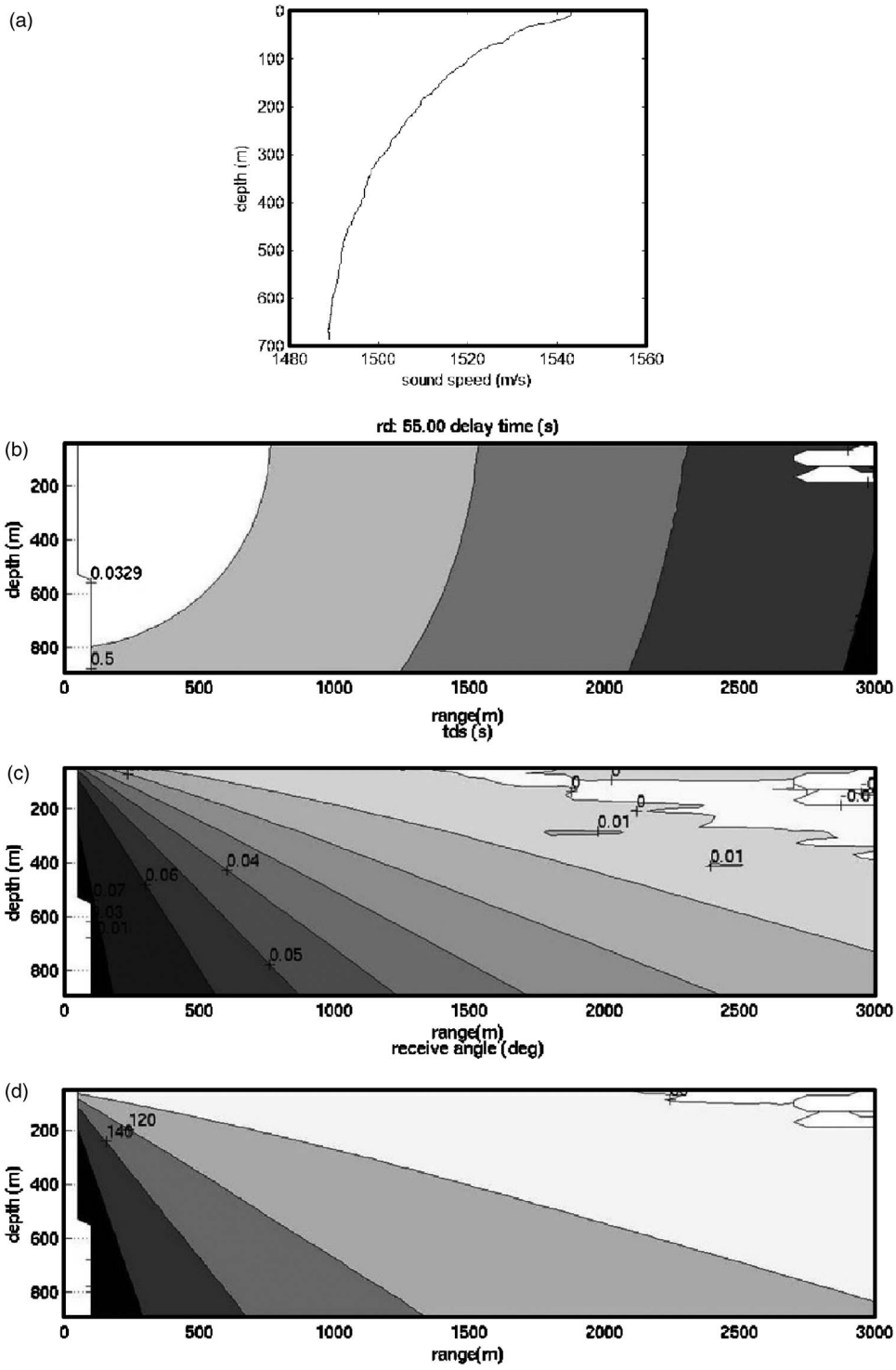

FIG. 3. (a) Downward-refracting sound speed profile measured on June 13, 2004. (b)–(d) Effect of sound speed profile on localization parameters, for a receiving hydrophone at 55 m depth. (b) Ray path length vs source range and depth; (c) direct-surface time delay vs source range and depth; (d) received ray elevation angle vs source range and depth. Note the appearance of a "shadow" zone beginning at shallow depths at 2 km range.

receiver depth of 55 m. The path-length contour map, which would consist of concentric circles in a constant-speed (isovelocity) profile, shows that the greatest horizontal range a receiver can detect a direct path from a surface source is 2.8 km in the GOM. Beyond this range, a source would have to be at progressively deeper depths to be detected via its direct path. The elevation angle contour map in the bottom subplot also illustrates this tendency.

Given that the duration of a sperm whale click is on the order of 10 ms, distinguishing t_{ds} values below this value becomes problematic, although cepstral methods can be successfully applied.[12,16–18] The contour map of t_{ds} shows that beyond 2.0 km range the direct-surface arrival time difference exceeds 10 ms only for sources deeper than 200 m, and the required source depth to attain this minimum interval increases with greater range. In general the deeper the receiving hydrophone, the greater the range over which the depth and horizontal range components of an animal's location can be teased apart.

The computations shown in Fig. 3 were repeated for receiving hydrophone depths from 15 m to 80 m, increasing in 5 m increments.

IV. EXPERIMENTAL SETUP

A. Equipment and deployment

A dedicated towed "tandem" array for the SWSS 3D tracking project was built between December 2003 and May 2004, and deployed during the SWSS 2004 cruise between May 27 and June 17, 2004 (Fig. 2). Designed according to the geometry in Fig. 1, the tandem array consists of two calibrated subarrays of three elements each, separated by $L = 200$ m of cable, with an additional 200 m of lead-in to the deck winch. Thus the rear subarray is deployed 400 m behind the ship stern. The 200 m aperture would be sufficient for tracking animals within 1–2 km of the vessel, based on a consideration of Eq. (6). An underwater connector (square in Fig. 2) at the base of the first array permits the arrays to be interchangeable, or even converted into two single arrays, providing emergency redundancy for the S-tag cruise requirements. Both subarrays incorporate pressure sensors, and a breakout box provided separate acoustic and pressure outputs. Each hydrophone on the tandem array has between −165 to −170 dB re 1 V sensitivity, with a flat frequency response between 100 Hz to over 24 kHz, although usable signal could be obtained past 30 kHz. The presence of a third hydrophone in each subarray provides redundancy in case of a sensor failure. An estimated total of 30 lb. of lead forms were added to the cable about 50 m ahead of the forward subarray to increase the array tow depths. For example, at 3 knots (around 2 m/s) the tow depth for the forward array was 30 m and the rear array about 55 m.

Between June 12 and June 18 two autonomous inclinometer packages were attached to both the forward and rear subarray to provide independent measurements of α_{local}, thus determining whether the simplified Eq. (6) was adequate for most situations. A second array, provided by Ecologic Inc., was deployed off the port side of the Gyre (Fig. 2). When combined with data from the rear subarray of the tandem array, acoustic observers were able to distinguish port/starboard ambiguities in the bearings without having to alter vessel course.

Data from two hydrophones in the forward array and two hydrophones in the rear array were filtered using a Khron-hite model 3944 filter/amplifier before being recorded onto an Alesis ADAT HD24XR hard disk digital recorder, along with two channels from the Ecologic array. Thus a total of six hydrophones were sampled at 96 kHz and stored in 24 bit WAV format. The start time of each recording was entered into both an Excel spreadsheet and a Microsoft Access database. The signal was high-pass filtered above 100 Hz to eliminate potential dc and 60 Hz line noise. The two pressure sensors were sampled by two process indicators in the breakout box, with output both a digital LED display and a serial port signal. The serial port signals were sampled by a Labview program on a dedicated laptop, which saved the time-stamped data to file.

B. Automated parameter extraction

The data were post-processed after the cruise, using automated procedures for extracting the localization parameters, similar to those discussed in Ref. 12. The recorded data were first rearranged into two stereo audio files, one for each subarray. The bioacoustic analysis software Ishmael[19] then detected impulses by monitoring the spectral energy content between 4 kHz and 15 kHz, and activating a MATLAB subroutine that identified whether a particular pulse was a direct arrival or a surface-reflected path. A direct path was identified as any pulse that was not preceded by another pulse during the previous 50 ms, which would be a typical value of $t_{ds,r}$ given the array depths and whale ranges considered here. Even when multiple animals are vocalizing, the odds of two direct path arrivals being detected within 50 ms of each other were small enough that direct-path arrivals from animals calling simultaneously could be distinguished. Pulse detections with acoustic bearings of less than 25 degrees were also rejected, in order to remove impulsive sounds generated by the tow vessel. For each direct-path detection, the MATLAB script estimated the acoustic bearing via standard cross-correlation methods, and then computed $t_{ds,r}$ simply by assuming the next detected pulse after a direct-path arrival was the surface-reflected path.

Once both subarrays had been processed this way, a second MATLAB script examined each direct-path arrival time on the rear subarray, and for every such "focal" click determined an appropriate set of interclick-intervals (ICIs) for that particular animal, by identifying other direct paths within a 10 second window that arrived within 10° of the acoustic bearing of the focal click. The program then scanned the direct-path arrivals on the forward subarray for a similar ICI pattern. Once a matching ICI set was found, the arrival-time difference t_{dd} for the direct path was determined. This "rhythm analysis" is a standard technique for many sperm whale acoustic analysis programs over widely spaced apertures.[1,14,20,21]

The hydrophone depths and cable inclination, which had been sampled every 10 seconds, were interpolated to assign a value to each direct-path arrival. Equations (5) and (6) then provided a slant range, and Eq. (1) a depth. As a check that the array cable is laterally straight, the values of $\eta_{d,f}$ and $t_{ds,f}$ were derived and compared with the measurements on the forward array. Navigation data from the ship GPS was also plotted to check whether the ship was changing course or speed during the time of interest.

V. RESULTS

A. Confirmation of tracking approach using bottom-reflected data and inclinometer measurements

Acoustic data were collected from the tandem array from May 27 through June 17, 2004. A particularly clean dive sequence from a single whale at close range was recorded on June 16, shortly before midnight of the last full cruise day. Numerous bottom-reflected returns were audible throughout the dive, making this data set a good candidate for an initial check of the tracking sequence. A MATLAB graphical-user interface (GUI) was written to permit convenient review of spectrograms from the forward and rear array simultaneously, and Fig. 4 shows a few seconds from the data set. Surface reflections are clearly visible on both sub-

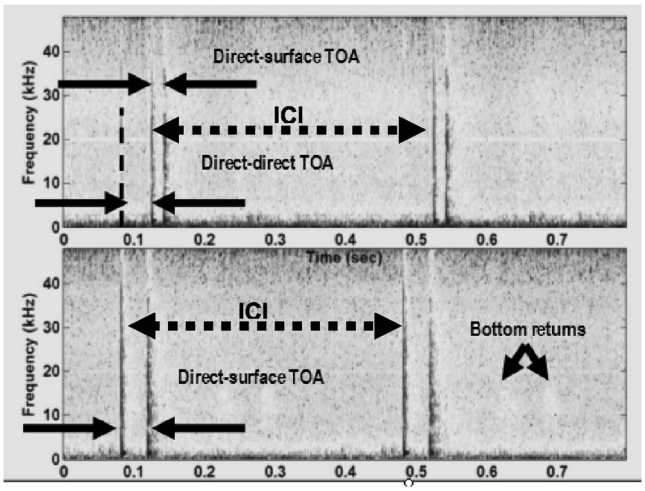

FIG. 4. Spectrograms of data collected during 2004 3D tracking experiment, as viewed with a MATLAB graphical user interface. All time units are in seconds. The top and bottom spectrograms (48 kHz sample rate, 1024 pt. FFT samples, 75% overlap) image data from the forward and rear subarrays. Up to five pieces of information can be obtained from each individual click, the differences between the arrival times of the direct and surface-reflected paths on the forward ($t_{ds,f}$) and rear ($t_{ds,r}$) hydrophones, the arrival time difference between the direct arrivals on both hydrophones (t_{dd}), and the acoustic bearings of both signals ($\eta_{d,f}$ and $\eta_{d,r}$). If both hydrophone depths are known, the animal's position can be fixed. Also shown is the interclick interval (ICI), which is used to identify the same whale on both hydrophones; and bottom-reflected paths, which permit an independent check of the tracking algorithm.

arrays, as are bottom-reflected returns. The interclick interval is shorter than the travel time of the bottom-reflected returns.

Figure 5 shows the output of the automated parameter detection routines. The $t_{ds,r}$ value for the whale in question

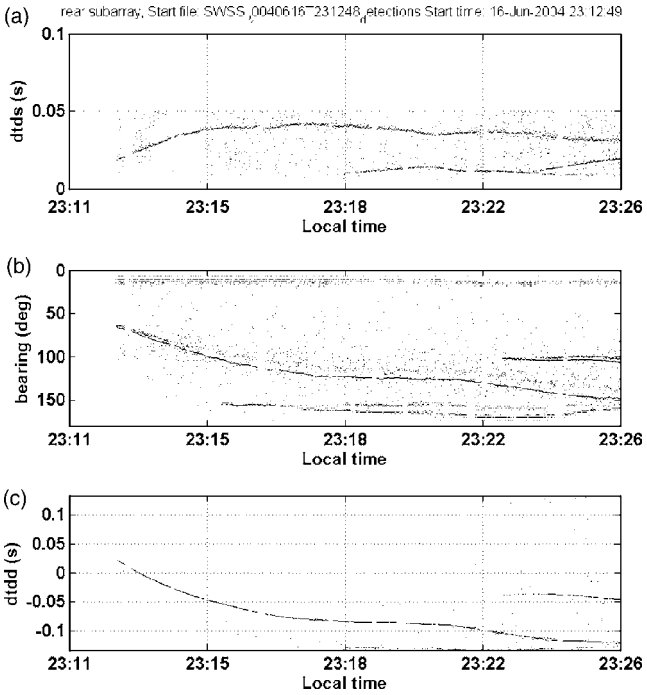

FIG. 5. Tracking parameters extracted automatically from the acoustic data on June 16. (a) Arrival time difference between the direct and surface-reflected sound arrivals on the rear subarray; (b) acoustic bearings measured on the rear subarray; and (c) arrival time difference t_{dd} between the forward and rear subarrays.

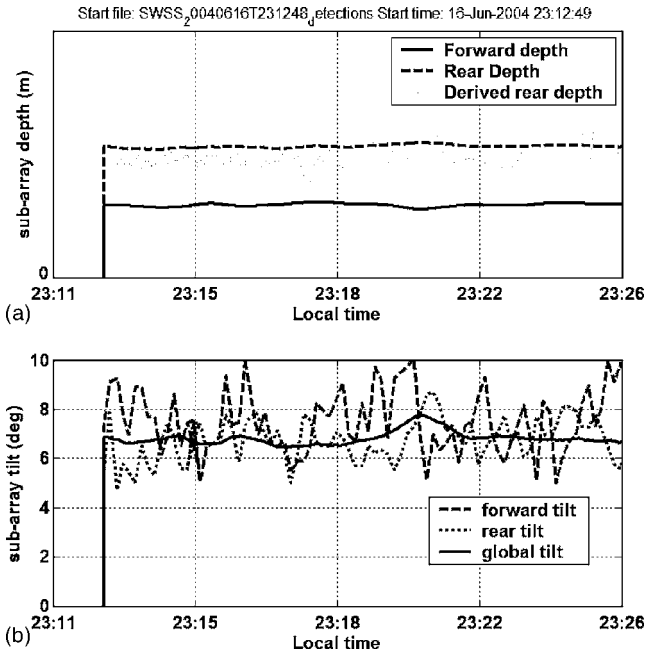

FIG. 6. Measurements of tandem array tow shape during the same time interval shown in Fig. 5. (a) Subarray depths of the forward (solid line) and rear (dashed line) subarrays, as measured by embedded pressure transducers. Rear subarray depths are also independently derived using bottom-reflected sperm whale clicks (hollow squares). (b) Comparison of α_{local} and α_{global} of tandem array. The local tilt was measured on the forward (dashed line) and rear (dotted line) subarrays. The global tilt (solid line) was derived from array depths in (a).

reaches nearly 50 ms at 23:17, then decreases as the array passes the whale, as is seen by the plots of acoustic bearing and t_{dd} shown in Figs. 5(b) and 5(c), respectively. Measurements of $t_{ds,r}$ less than 10 ms are not attempted.

Figure 6 shows independent checks of the geometry of the towed array cable. The top subplot shows the measured depths of the two subarray pressure transducers, along with rear subarray depths derived from bottom-reflected returns. The measured and derived rear subarray depths are within a few meters of each other. The bottom subplot compares the output of the inclinometers, which directly measure α_{local}, with the value of α_{global} derived from the hydrophone depths and knowledge of the cable length. Despite the large variance in the inclinometer readings, the mean values of α_{local} are within a degree of α_{global}, indicating that the array cable is relatively straight, and that Eq. (6) is valid for the cable at this tow speed. Measurements at other times and other ship speeds indicate that setting $\alpha_{\text{local}} \sim \alpha_{\text{global}}$ is a good approximation.

Figure 7 shows range and depth fixes using the single-phone localization procedure described in Ref. 8, along with the tracking results derived in Sec. II. Until 23:19 the results agree extremely well as the animal dives from 100 m down to 550 m. After this time, however, the single-phone measurements indicate that the animal remains at depth, while the tracking method introduced here determines that the animal's range and depth decreases substantially—effectively, that the path length $P_{d,r}$ is decreasing. The answer to this inconsistency appears in the bottom subplot, which plots the ship speed in knots and the vessel course over ground (COG)

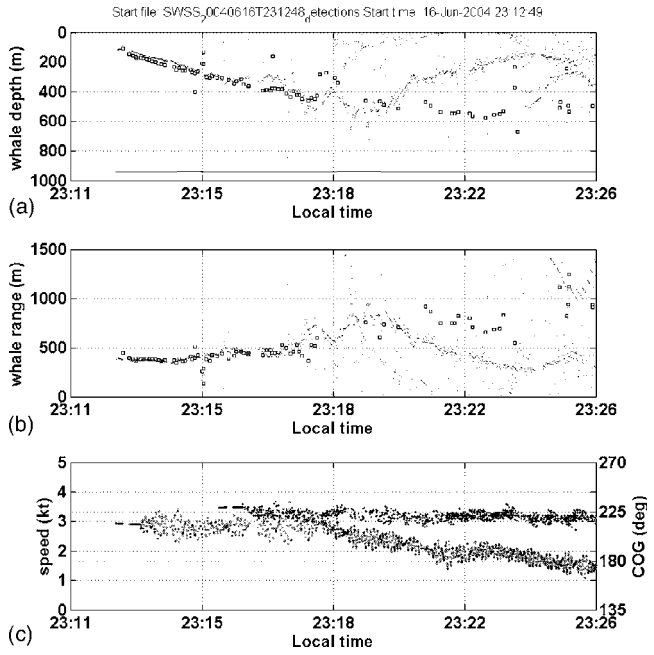

FIG. 7. Analytic range-depth track estimates, using data beginning at June 16, 2004, 11:13 CDT, covering the same time period as Figs. 5 and 6. Positions derived using methods derived in Sec. II are shown as dots, and positions derived by exploiting bottom multipath on a single hydrophone as shown by squares. The whale depths are shown in (a), the horizontal ranges from the forward hydrophone are shown in (b), and (c) shows the ship speed (plus signs) and course over ground (circles) measured by GPS over the same interval. Note divergence of tracking methods when ship course changes at 23:17.

in degrees. At 23:19 the ship begins a 40 degree port turn that continues past 23:37. This turn throws the tow cable out of a two-dimensional vertical plane, violating the assumptions of Sec. II. Thus the course of the towing vessel must be monitored carefully for the tracking techniques presented here to work.

B. Effect of ray refraction

Applying the numerical ray-refraction tracking procedure to Fig. 7 did not yield any substantial differences from the analytical formulas. However, clicks generated by animals at ranges greater than 1 km show effects of ray refraction. To illustrate this, Fig. 8 shows a 30 minute tracking segment from June 8, 2004, using the analytic formulas. The bottom subplot illustrates that the ship course and speed were steady through the encounter. Although it is difficult to distinguish, two animals are present at the same depth in the first half of the sequence, while one animal is present in the latter half. Figure 9 shows the same data analyzed using the numerical procedure outlined in Sec. III. Comparing plots reveals that at horizontal ranges greater than roughly 1 km animals that appear to be at 300–400 m depth using the analytic formulas are actually 100 m deeper when an accurate propagation model is taken into account. This example demonstrates that as tracking is extended to greater ranges, the effects of the depth-dependent sound speed profile cannot be neglected if accurate dive depths of animals are to be inferred from passive acoustics.

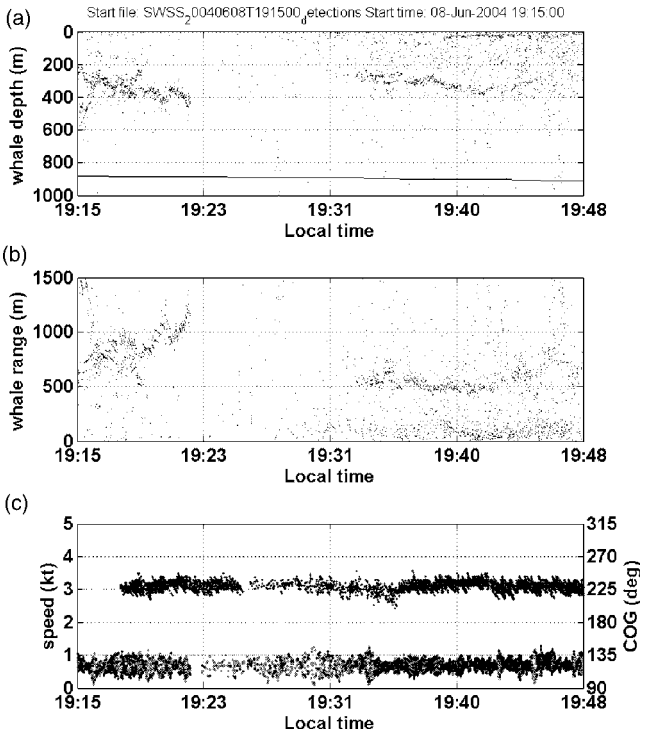

FIG. 8. Same as Fig. 7, except analytically derived tracks are shown for three whales beginning June 8, 19:15 local time.

C. Foraging depths over several days

A selection of the 2004 data have been selectively analyzed to determine depth ranges of individual animals over a 10 day period, during times where the ship course and speed is constant over long periods. Table II shows the results of measured foraging depths, with an asterisk indicating that at least part of an animal's initial dive profile was detected. This is not meant to be an exhaustive list of encounters, but a selection intending to show the diversity of the dive depths encountered during the cruise. Many of these measurements

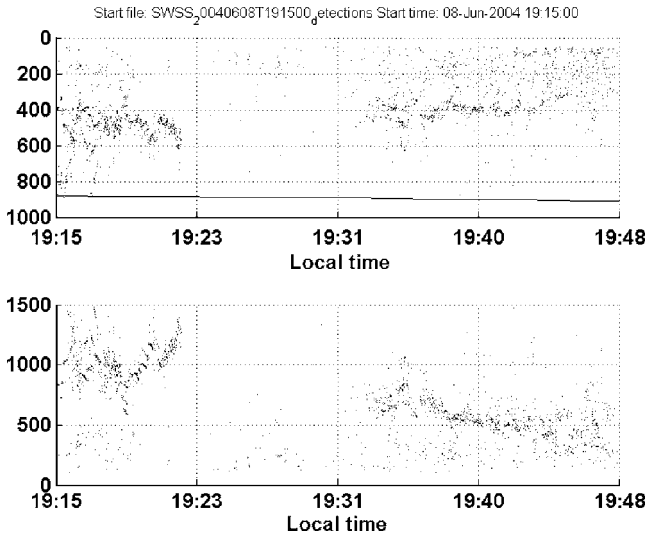

FIG. 9. Same as Fig. 8, but tracks are derived using the numerical procedure discussed in Sec. III. At horizontal ranges greater than 1 km, the effects of ray refraction due to a depth-dependent sound speed profile are not negligible.

TABLE II. Depths traversed by individual whales during SWSS 2004 cruise, corrected for ray-refraction effects. Times are rounded to the nearest 5 minute increment, and depths to the nearest 50 m increment (the depth uncertainty from Table I). A single depth is shown if an animal remained within ±50 m of that depth. Ship coordinates shown are the ship location midway through the dive profile measurement. An asterisk (*) indicates the observation of what appears to be an initial dive descent.

Date	Time	Latitude	Longitude	Depth range(m)	Description
June 7	8:38–9:30	28.112	−89.800	400–600 m	
June 7	11:30–12:00	28.154	−87.707	250 m	
June 8	16:45–17:45	28.274	−89.584	200–300 m	
June 8	16:40–17:30	Same	Same	300–400 m	
June 8	18:00–18:10	28.316	−89.596	200 m	
June 8	18:00–18:30	Same	Same	200–400 m	
June 8	18:30–19:00	Same	Same	300 m	
June 8	19:15–19:20	28.327	−89.538	350–600 m*	Section IV B
June 8	19:15–19:25	Same	Same	400–500 m	
June 8	19:35–19:45	Same	Same	400 m	
June 13	19:55–20:00	28.267	−89.578	250 m	
June 13	20:00–20:10	Same	Same	300 m	
June 13	20:10–20:15	Same	Same	400 m	
June 13	22:15–22:25	28.287	−89.573	200–400 m	
June 13	22:40–23:00	Same	Same	400–500 m	
June 16	13:25–13:30	Same	Same	300 m	
June 16	16:30–16:55	28.163	−89.382	200–450 m	
June 16	16:45–17:05	Same	Same	350 m	
June 16	16:40–17:05	Same	Same	300–500 m	
June 16	16:45–17:10	Same	Same	200–400 m	
June 16	23:15–23:20	28.000	−89.584	150–500 m*	Section IV A
June 17	1:15–1:20	27.99	−89.590	150–450 m	
June 17	1:25–1:30	Same	Same	250–400 m	
June 17	16:05–16:20	28.178	−89.632	150–350 m	
June 17	16:45–17:00	Same	Same	300 m	

were taken during the night or during days of poor weather, whenever tagging activities and visual observations were infeasible.

During these time periods, the range-depth tracks of animals are computed using both the methods of Sec. II and the refraction-corrected methods of Sec. III, but only the refraction-corrected results are shown here. The derived animal depths are rounded to the nearest 50 m, on the basis of the sensitivity analysis presented in Table I. The quality of the tracks obtained improved as the acoustic observers gained more experience in directing the vessel course and speed. By June 16 and 17, up to three animals could be tracked simultaneously using the system.

VI. CONCLUSION

An automated 3D passive acoustic tracking system has been developed and tested on a 200 m aperture towed array system built specifically for this purpose, and animals out to 1.5 km range have been successfully tracked. Information from bottom-reflected returns and additional parameters measured from the forward subarray has been used to confirm the tracking results when possible. At ranges of around 1 km or greater, the effects of a depth-dependent sound speed profile must be incorporated into the tracking procedure to obtain accurate results. In addition, the ship course must be steady and true to avoid large localization biases.

Direct inclinometer measurements of the tow cable dynamics have revealed that under many conditions the cable's vertical curvature is small, permitting substantial simplification of the analytical formulas. However, the sensitivity analysis presented in Table I indicates that small changes in local tilt can cause large variations in estimated animal depth when the animal is either directly ahead or behind the system. The technique presented here thus complements the procedure outlined in Ref. 12, which works best when an animal is directly ahead of or behind a vessel.

Further refinements in modeling the tow cable dynamics are expected, to determine under what circumstances precise information about the cable sag would be required. Eventually data collected using these techniques may not only find use in marine mammal mitigation efforts, but might also be combined with measurements of acoustic backscattering depths to gain insight into foraging ecology.

ACKNOWLEDGMENTS

The author thanks Bruce Mate of Oregon State University for permitting the deployment of the tracking system for the summer S-tag cruise, and the Industrial Research Funders Coalition (IRFC) for providing support to build the towed array system. Tom Norris, Elizabeth Zele, Sarah Tsoflias, and Alyson Azzara helped monitor and record acoustic data during that cruise. Matt Howard of Texas A&M provided data on the water depth beneath the R/V Gyre in 2004. This work

was supported by the U.S. Minerals Management Service, under Cooperative Agreement 1435-01-02-CA-85186. Ann Jochens and Doug Biggs of Texas A&M University helped arrange this support, and have been supportive of this research since its inception.

[1]R. Leaper, O. Chappell, and J. Gordon, "The development of practical techniques for surveying sperm whale populations acoustically," Rep. Int. Whal. Comm. **42**, 549–560 (1992).
[2]J. Barlow and B. L. Taylor, "Estimates of sperm whale abundance in the northeastern temperate Pacific from a combined acoustic and visual survey," Marine Mammal Sci. **21**(3), 429–445 (2005).
[3]J. Gordon, D. Gillespie, J. Potter, A. Frantzis, M. P. Simmonds, R. Swift, and D. Thompson, "A review of the effects of seismic surveys on marine mammals," Mar. Technol. Soc. J. **37**, 16–33 (2004).
[4]D. Gillespie, "An acoustic survey for sperm whales in the Southern Ocean Sanctuary conducted from the RSV Aurora Australis," Rep. Int. Whal. Comm. **47**, 897–907 (1997).
[5]H. Whitehead, *Sperm Whales: Social Evolution in the Ocean* (University of Chicago Press, Chicago, 2003).
[6]J. C. Gordon, "The behavior and ecology of sperm whales off Sri Lanka," Ph.D. thesis, University of Cambridge, Cambridge, UK, 1987.
[7]B. Møhl, M. Wahlberg, P. T. Madsen, L. A. Miller, and A. Surlykke, "Sperm whale clicks: Directionality and source level revisited," J. Acoust. Soc. Am. **107**, 638–648 (2000).
[8]A. Thode, D. K. Mellinger, S. Stienessen, A. Martinez, and K. Mullin, "Depth-dependent acoustic features of diving sperm whales (Physeter macrocephalus) in the Gulf of Mexico," J. Acoust. Soc. Am. **112**, 308–321 (2002).
[9]W. M. X. Zimmer, P. L. Tyack, M. P. Johnson, and P. T. Madsen, "Three-dimensional beam pattern of regular sperm whale clicks confirms bentthorn hypothesis," J. Acoust. Soc. Am. **117**, 1473–1485 (2005).
[10]J. J. Nooteboom, "Signature and amplitude of linear airgun arrays," Geophys. Prospect. **26**, 194–201 (1978).
[11]S. Vaage and B. Ursin, "Computation of signatures of linear airgun arrays," Geophys. Prospect. **35**, 281–287 (1987).
[12]A. Thode, "Tracking sperm whale (Physeter macrocephalus) dive profiles using a towed passive acoustic array," J. Acoust. Soc. Am. **116**, 245–253 (2004).
[13]C. R. Greene and M. W. McLennan, *Passive Acoustic Localization and Tracking of Vocalizing Marine Mammals Using Buoy and Line Arrays* (Hobart, Tasmania, 1996).
[14]J. Ward, M. Fitzpatrick, N. DiMarzio, D. Moretti, and R. Morrissey, "New algorithms for open ocean marine mammal monitoring," *OCEANS 2000 MTS/IEEE Conference and Exhibition. Conference Proceedings (Cat. No. 00CH37158)* (IEEE, Piscataway, NJ, 2000), pp. 1749–1752.
[15]C. O. Tiemann, M. B. Porter, and L. N. Frazer, "Localization of marine mammals near Hawaii using an acoustic propagation model," J. Acoust. Soc. Am. **115**, 2834–2843 (2004).
[16]W. M. X. Zimmer, M. P. Johnson, A. D'Amico, and P. L. Tyack, "Combining data from a multisensor tag and passive sonar to determine the diving behavior of a sperm whale (Physeter macrocephalus)," IEEE J. Ocean. Eng. **28**, 13–28 (2003).
[17]A. V. Oppenheim and R. W. Schafer, *Discrete-Time Signal Processing* (Prentice-Hall, Englewood Cliffs, NJ, 1989).
[18]J. M. Tribolet, *Seismic Applications of Homomorphic Signal Processing* (Prentice-Hall, Englewood Cliffs, NJ, 1979).
[19]D. K. Mellinger, "Ishmael 1.0 User's Guide," NOAA/PMEL Tech. Mem. Report PMEL-120, 2002.
[20]R. J. Barton III, S. Jarvis, R. J. Rowland, and D. Moretti, "The application of EZ-Gram sonar display aids to the Marine Mammal Monitoring on Navy Undersea Ranges (M3R) system," *Oceans 2002 Conference and Exhibition. Conference Proceedings (Cat. No. 02CH37362)* (IEEE, Piscataway, NJ, 2002), Vol. **2**, pp. 1064–1070.
[21]D. Gillespie and R. Leaper, "Detection of sperm whales (Physeter macrocephalus) clicks, and discrimination of individual vocalisations," Eur. Res. Cetaceans **10**, 87–91 (1997).